

## Response to Gloria Manney and Michelle Santee

We thank Gloria Manney and Michelle Santee for their extensive comments. Kindly find below our responses to each (quoted between []). We hope that our responses will clarify the main issues they have addressed. In particular, we hope that with the changes made, also in reply to the two anonymous reviewers, we have made more convincing that the IASI HNO<sub>3</sub> dataset has the potential to contribute to stratospheric studies in general, and to the time evolution of the polar processes in particular.

### General comment

Throughout this manuscript, starting with its title, the term “denitrification” is taken to be synonymous with the uptake of gas-phase HNO<sub>3</sub> through the formation of PSCs. Although not without precedent, this approach is contrary to common practice and may lead to confusion. Condensation of HNO<sub>3</sub> in PSCs is usually referred to as “sequestration”, while the term “denitrification” is usually reserved for the permanent removal of HNO<sub>3</sub> from the lower stratosphere through the sedimentation of PSCs. In the absence of analysis of direct PSC measurements (e.g., from an instrument such as CALIOP), the occurrence of true denitrification can only be inferred from space-borne measurements of gaseous HNO<sub>3</sub> when abundances do not rebound as PSCs dissipate at the end of winter, suggesting permanent removal. Thus the “drop temperature” derived in this study is indicative only of the onset of PSC formation, not the onset of denitrification, as is stated in numerous places in the paper.

We agree that, from IASI, we can only detect a “removal from the gas phase”, caused by sequestration into particles with or without sedimentation. This misuse of the term “denitrification” was also highlighted by the two anonymous referees. Careful attention has been given in the manuscript to avoid abusive use of the term “denitrification”. Hence, “onset of HNO<sub>3</sub> denitrification” has been changed to “the onset of HNO<sub>3</sub> depletion” in L.169 and where appropriate in the revised manuscript. The title has also been changed accordingly to: “Polar stratospheric HNO<sub>3</sub> depletion surveyed from a decadal dataset of IASI total columns”.

### Specific comments

[Abstract: L2: It is misleading (particularly for those who read only the abstract of the paper) to characterize the IASI HNO<sub>3</sub> total columns as having “good vertical sensitivity”. Indeed, this optimistic assessment is directly contradicted in Section 2, where IASI is stated to have “low vertical sensitivity ... with only one independent piece of information” (L76).]

As stated in the text, we here refer to “a good vertical sensitivity in the low and middle stratosphere”, not to a good vertical resolution of the measurement. Note that HNO<sub>3</sub> vertical profiles are retrieved from IASI measurements, not simply total columns. Hence, even if the sensitivity covers the entire altitude range from the troposphere to the stratosphere with no clear decorrelation (DOFS~1) between the retrieved layers, it is shown in Ronsmans et al. (2016) that the highest sensitivity lies in the low-middle stratosphere, depending on latitude and season (from ~70 to 30 hPa within the cold Antarctic winter). This means that the variability in the measured total column is mainly representative of that layer. “low vertical sensitivity” in L76 has been changed to “low vertical resolution” to be more in line with the above.

We agree that the IASI sensitivity was insufficiently put forward in the text. We made it more explicit at several places in the revised manuscript; e.g. in Section 1: “IASI provides reliable total column measurements of HNO<sub>3</sub> characterized by a maximum sensitivity in the low-middle stratosphere around 50 hPa (20 km) during the dark Antarctic winter (Ronsmans et al., 2016;

2018) ...” and in Section 2: “... the largest sensitivity of IASI in the region of interest, i.e. in the low and mid-stratosphere (from 70 to 30 hPa), where the HNO<sub>3</sub> abundance is the highest (Ronsmans et al., 2016).

[Introduction: L48-49: It should be made more clear that this is by no means an exhaustive list of spaceborne instruments that have measured stratospheric HNO<sub>3</sub>.]

The study of Santee et al. (1999) on MLS/UARS measurements has been added:

“Several satellite instruments measure stratospheric HNO<sub>3</sub> (e.g. MLS/Aura (e.g. Santee et al., 2007), MIPAS/ENVISAT (Piccolo 50 and Dudhia, 2007), ACE-FTS/SCISAT (Sheese et al., 2017) and SMR/Odin (Urban et al., 2009)).”

[Section 2: The information provided about the IASI HNO<sub>3</sub> retrieval, data quality, and data screening is insufficient. This information is critical to assessing the robustness of the reported results, and readers should not be forced to refer to previous papers to find it.]

The reader is here invited to refer to the figure 4 of Ronsmans et al. (2016) which illustrates the global distribution of the total retrieval error for HNO<sub>3</sub> (integrated over 5 to 35 km) separately for January (left) and July (right) over the period of the IASI measurements. The mid- and polar latitudes are characterized by low total retrieval errors of around ~3-5% - which corresponds to a reduction by a factor of 18-30 compared to the prior uncertainty (90%) and indicates a real gain of information – except above Antarctica during wintertime where the errors reach 25%. They are explained by (1) a weaker sensitivity (i.e. a larger smoothing error which represents in all cases the largest source of the retrieval error) above such cold surface (DOFS of ~0.95 within the dark Antarctic vortex – see figure 3 of Ronsmans et al., 2016) and by (2) a misrepresentation of the wavenumber-dependent surface emissivity above ice surface (Hurtmans et al., 2012). As also required by the two anonymous referees, this is now made more explicit in Section 2 of the revised manuscript:

“The total columns are associated with a total retrieval error ranging from around 3% at mid- and polar latitudes to 25% above cold Antarctic surface during winter (due to a weaker sensitivity above very cold surface with a DOFS of ~0.95 and to an poor knowledge of the seasonally and wavenumber-dependent emissivity above ice surfaces which induces larger forward model errors), and a low bias (lower than 12%) in polar regions over the altitude range where the IASI sensitivity is largest, when compared to ground-based FTIR measurements (see Hurtmans et al., 2012; Ronsmans et al., 2016 for more details).”

Note also that similarly to these two previous studies, HNO<sub>3</sub> measurements characterized by a poor spectral fit or by a low information content (DOFS < 0.9) have been filtered out of this analysis. This is now clearly mentioned in Section 2 of the revised manuscript:

“Quality flags similar to those developed for O<sub>3</sub> in previous IASI studies (Wespes et al., 2017) were applied a posteriori to exclude data (i) with a corresponding poor spectral fit (e.g. based on quality flags rejecting biased or sloped residuals, fits with maximum number of iteration exceeded), (ii) with less reliability (e.g. based on quality flags rejecting suspect averaging kernels, data with less sensitivity characterized by a DOFS lower than 0.9) or (iii) with cloud contamination (defined by a fractional cloud cover larger than 25 %).”

[In later sections (e.g., L186, L225), errors in IASI retrievals arising from issues with emissivity above ice shelves are invoked to account for some dubious results, but no mention of these

poor-quality retrievals is made in the “Data” section, nor is it explained why quality-control measures fail to properly filter out these suspect data points.]  
See our response to the above comment.

Bright land surface such as desert or ice might in some cases lead to poor HNO<sub>3</sub> retrievals due to a poor knowledge of the wavenumber-dependent emissivity above such surfaces, which can alter the retrieval by compensation effects (Wespes et al., 2009). FORLI relies on the monthly climatology of surface emissivity built by Zhou et al. (2011) from several years of IASI measurements on a 0.5x0.5 grid and for each 8461 IASI spectral channels when available, or on the MODIS climatology that is unfortunately restricted to only 12 channels in the IASI spectral range; see Hurtmans et al. (2012) for more details. Although wavenumber-dependent surface emissivity atlases are used in FORLI, it is clear that this parameter remains critical and causes poorer retrievals that, in some instances, pass the posterior filtering. The total HNO<sub>3</sub> columns over eastern Antarctica which show drop temperatures much above 195K might precisely be related to this. We have made this clear in Section 4.2 of the revised version:

“...emissivity features that are known to yield errors in the IASI retrievals. Indeed, bright land surface such as ice might in some cases lead to poor HNO<sub>3</sub> retrievals. Although wavenumber-dependent surface emissivity atlases are used in FORLI (Hurtmans et al., 2012), this parameter remains critical and causes poorer retrievals that, in some instances, pass through the series of quality filters and affect the drop temperature calculation.”

[L78: 10 km can hardly be characterized as the “mid-stratosphere”.]

It has been corrected:

“... in the low and mid-stratosphere (from ~70 to ~30 hPa),...”

[L84: “normal” has a specific statistical meaning and is not the appropriate word here.]

The reviewers are right; “normal” has been removed.

[L85-86: The validity of the analysis approach depends on the 50 hPa pressure surface and the 530 K isentropic surface being in very close proximity during Antarctic winter. This implicit assumption should be explicitly justified in the paper.]

Figure 1 below represents the figure 2 of the manuscript but for the temperature at 30 hPa (top panel) and 70 hPa (bottom panel) for the sake of comparison. As expected, the drop temperatures are the lowest when using the temperatures at 30 hPa. They vary from 185-195 K (~192K on average) at 30 hPa to 195-204 K (~198 K on average) at 70 hPa with values of ~189-202 K (~194 K on average) at 50 hPa.

As explained in the manuscript, the use of the 195 K at 50 hPa as single level for the analysis is justified by the fact that it corresponds best to the maximum of IASI vertical sensitivity during the polar night (see Figure 3 of Ronsmans et al. 2016 and responses to related comments above); another justification is found a posteriori by the consistency between the 195 K threshold temperature taken at 50 hPa and the onset of the strong total HNO<sub>3</sub> depletion seen by IASI, which matches the NAT development that occurs in June around that level. However, we fully agree that the HNO<sub>3</sub> abundances over a large part of the stratosphere (between 70 and 30 hPa) contribute to the total HNO<sub>3</sub> variations detected by IASI and that this inevitably affects the drop temperature calculation at 50 hPa. In order to address this issue and as also requested by referee #1, we have added in the manuscript the range of drop temperatures when calculated at these

two other pressure levels (from 185 K to 204 K); this indeed allows the reader to better judge on the uncertainty of the drop temperature at 50 hPa (189-202 K). The text in the revised manuscript is changed to:

“... Nevertheless, given the range of maximum IASI sensitivity to HNO<sub>3</sub> around 50 hPa, typically between 70 and 30 hPa (Ronsmans et al., 2016), the drop temperatures are also calculated at these two other pressure levels (not shown here) to estimate the uncertainty of the calculated drop temperature defined in this study at 50 hPa. The 30 hPa and 70 hPa drop temperatures range respectively over 185.7 K – 194.9 K and over 194.8 K – 203.7 K, with an average of 192.0 +/- 2.9 K and 198.0 +/- 3.2 K (1 $\sigma$  standard deviation) over the ten years of IASI. The average values at 30 hPa and 70 hPa fall within the 1 $\sigma$  standard deviation associated with the average drop temperature at 50 hPa. It is also worth noting the agreement between the drop temperatures and the NAT formation threshold at these two pressure levels (T<sub>NAT</sub> ~193 K at 30 hPa and ~197 K at 70 hPa) (Lambert et al., 2016).”

See comment here below for the justification of a single theta level (530 K) for the PV.

[L89-91: It is highly problematic to use a single theta level to distinguish inside from outside vortex regions for column measurements. This approach implicitly (and erroneously) assumes that the vortex does not tilt, shrink, or expand with height over the altitude range considered. A better approach would have been to check PV over a range of levels and discard measurements classified as outside the vortex at any one of those levels. A similar comment can be made concerning the use of a single pressure level for temperature. Again, it might have been better to use a range of T over the ~10–30 km layer where IASI has most sensitivity. Some attempt is made to justify the latter choice (using 195 K at 50 hPa) in Section 3 (L141-142) and Section 4 (L168-169), but the arguments are not convincing, as the authors themselves appear to recognize when they state (L188-189) “hence, the use of temperature at a single pressure level might be restrictive to some extent”.]

Here again, the approach that we have followed was to select the levels that correspond best to the altitude of IASI maximum vertical sensitivity during the polar night (see Figure 3 of Ronsmans et al. 2016 and responses to related comments above). We agree, however, that considering PV over the range of the largest IASI sensitivity (from ~30 to ~70 hPa during the polar night) would allow the reader to better judge on the uncertainty of our approach. To that end, the figure 2 below compares the maps of PV at 475 K (~65 hPa), 530 K (~50 hPa) and 600 K (~30 hPa) over the southern latitudes averaged over the period 15 May – 15 July (period of drop temperatures detection inside the inner vortex core) for the year 2008. They show quite similar shape of the vortex over the altitude of maximum IASI sensitivity which, hence, has only small influence on our delimitation of the inner polar vortex (delimited by a PV value of  $-10 \times 10^{-5} \text{K.m}^2.\text{kg}^{-1}.\text{s}^{-1}$  at 530 K) and, thus, on the detection of the drop temperature averaged inside that region (see Figure 2 of the manuscript). Note, furthermore, that our approach has no influence on the spatial distribution of the drop temperature illustrated in Fig.5 of the manuscript, which is independent of the PV.

See comment here above for the justification of the use of a single pressure level (50 hPa) for the temperature.

[Section 3: The definition of the three “regimes” in the T/HNO<sub>3</sub> relationship seems arbitrary and not well justified. For example, R1 is defined to begin in April, but Fig. 1a shows that

HNO<sub>3</sub> values start to increase rapidly and temperatures start to decrease rapidly in March (or even February, as noted in L117), not April. Only R2 encompasses a steep change in HNO<sub>3</sub>, but that regime also includes a lengthy period during which HNO<sub>3</sub> remains nearly constant. It might have been better to break R2 into an “onset of PSC formation” phase and a “denitrification plateau” phase. Moreover, as defined in the paper, R2 extends through, not to, September as stated in L108. These problems are evident in the discussion in this section, as in some cases the behavior ascribed to one regime actually occurs in another.]

The definition of the three “regimes” in the T/HNO<sub>3</sub> relationship made here is actually based on changes in both HNO<sub>3</sub> and T, not only in HNO<sub>3</sub>.

We did not state in our manuscript that “HNO<sub>3</sub> values start to increase rapidly and temperatures start to decrease rapidly in March (or even February, as noted in L117), not April”. In the manuscript, it is clearly stated in L117: “The plateau lasts until approximately February, where HNO<sub>3</sub> total column slowly starts increasing, reaching the April-May maximum in R1”. Our statement specifically justified the start of R1 in April.

We changed “R2 extends from June to September” to “R2 extends from June to October” in L108.

[L102 and Fig. 1 caption: The red line in Fig. 1a is horizontal, not vertical, and Fig. 1b contains no such line – it is on Fig. 1c. Neither red line is defined in the caption.]

For Fig. 1a: “horizontal” has been changed to “vertical”.

Fig. 1b and 1c do contain a red vertical line.

The red horizontal or vertical lines are now mentioned in the caption of the revised manuscript.

[L102 and Fig. 1: 2011 was a particularly cold and long-lasting Antarctic winter, and thus it is arguably not representative. Some explanation for why that year was selected for highlighting in Fig. 1b is needed.]

As expected from figure 1c, any other year could have been chosen instead of the year 2011 to illustrate the HNO<sub>3</sub> total columns versus temperatures (at 50 hPa) histogram in figure 1b. It is now clearly mentioned in the revised manuscript:

“Similar histograms are observed for the ten years of IASI measurements (not shown).”

[L105-106: The contribution of confined descent inside the developing vortex bringing air rich in HNO<sub>3</sub> from above into the domain where IASI is most sensitive has been ignored here – isn’t descent also a factor leading to the observed high HNO<sub>3</sub> total column values in early austral autumn?]

The domain where IASI is the most sensitive does actually cover the maximum HNO<sub>3</sub> concentrations, hence, the high HNO<sub>3</sub> total column values cannot be explained by the descent of HNO<sub>3</sub> rich air. However, in response to the two anonymous referees, the sentence has been rewritten as follows:

“These high HNO<sub>3</sub> levels result from low sunlight, preventing photodissociation, along with the heterogeneous hydrolysis of N<sub>2</sub>O<sub>5</sub> to HNO<sub>3</sub> during autumn before the formation of polar stratospheric clouds (Keys et al., 1993; Santee et al., 1999; Urban et al., 2009; DeZafra et al., 2001). This period also corresponds to the onset of the deployment of the southern polar vortex which is characterized by strong diabatic descent with weak latitudinal mixing across its boundary, isolating polar HNO<sub>3</sub>-rich air from lower latitudinal airmasses.”



[L115-116: In addition to a lack of citations of earlier papers on renitrification of the lowermost stratosphere (LMS), this sentence is not a very clear expression of the fact that IASI is not sensitive to the LMS and hence renitrification has little impact on the observed evolution of total column HNO<sub>3</sub>.]

The renitrification at lower stratospheric layers was merely mentioned here and it was not meant to be extensively reviewed. To address the comment, Lambert et al. (2012), which was already cited at several places of the manuscript has been added here. It is clearly stated in the revised version that a likely renitrification of the LMS could hardly be detected given the maximum sensitivity of IASI to HNO<sub>3</sub> at higher levels than those at which it occurs:

“The likely renitrification of the lowermost stratosphere (Braun et al., 2019; Lambert et al., 2012), where the HNO<sub>3</sub> concentrations and the IASI sensitivity to HNO<sub>3</sub> are lower (Ronsmans et al., 2016), cannot be inferred from the IASI measurements.”

[L119-121: Why is 2010 highlighted in Fig. 1a (green line)? Other recent Antarctic winters were also disturbed with some minor SSW activity, e.g., 2012 and 2013. Did those episodes not affect the HNO<sub>3</sub> distribution? Also, why does the green line show T at 20 hPa, when the other curves show T at 50 hPa? More explanation for why the authors chose to show this particular level for this particular year is needed.]

As explained in the text, 2010 is chosen because of its highest HNO<sub>3</sub> levels and highest temperatures within the Antarctic winter. No strong warming and related enhanced HNO<sub>3</sub> levels are observed from IASI for the years 2012 and 2013 (see Fig. 1a and Fig.4 of the manuscript). We have chosen to illustrate the temperature at 20 hPa for 2010 (dotted green line) in addition to the ones at 50 hPa (dashed lines) for each year simply because that level shows a distinct increase in temperature (cfr de Laat and van Weele, 2011) reflecting the presence of a SSW during the winter of 2010, while at 50 hPa, the increase in temperatures is smaller (dashed green line).

[Fig. 1c: In general this plot is not well explained or well motivated. By showing the position in temperature / HNO<sub>3</sub> space of the bin with the maximum number of observations, important information about the range of those values on a given day is omitted. The ranges in Fig. 1b suggest that the values at a given time may span most of the HNO<sub>3</sub> axis in Fig. 1c, rendering the curves shown less meaningful. In addition, it is stated (L127) that this figure highlights the interannual variability in total HNO<sub>3</sub>, but interannual variability is also clearly seen in panel (a), which is much easier to interpret. The discussion relates the picture in Fig. 1c to the three regimes, but since they are not marked on this panel, it cannot easily be examined without reference to Fig. 1a. It is therefore not obvious what additional value this figure brings to the paper.]

We agree that figure 1c does not bring additional information in comparison with the figures 1a and 1b; however, it is an original way to give insight into the HNO<sub>3</sub>/temperature cycle and, in that respect, it nicely complements figure 1a. We would not be in favour of removing it.

Regarding the other comment, it is true that the daily range of HNO<sub>3</sub> values around those of highest occurrence is not represented in Fig. 1c but note that it does not correspond to the range of HNO<sub>3</sub> values in Fig.1b which cover 3 months of IASI measurements. Hence, we do not agree with the comments that “The ranges in Fig. 1b suggest that the values at a given time may span most of the HNO<sub>3</sub> axis in Fig. 1c, rendering the curves shown less meaningful”. The daily

variability associated with the HNO<sub>3</sub> time series in the equivalent latitude bands can be found in Ronsmans et al. (2018).

In order to respond to the comment, the three regimes that were identified in Fig. 1a and Fig. 1b are now also indicated in Fig. 1c of the revised manuscript.

[L125: HNO<sub>3</sub> columns are said to slowly increase as the T decreases over “February to May, i.e., R3 to R1”. However, R3 is defined to start in October, and actually the slow increase in total HNO<sub>3</sub> starts before February, arguably even as early as December.]

Here again we would like to stress that we did not only consider the change in HNO<sub>3</sub>, but well the changes in both HNO<sub>3</sub> and temperature; HNO<sub>3</sub> columns do indeed increase as the temperature decrease over February to May but before February the HNO<sub>3</sub> levels increase as temperature also increase.

[L126: In the discussion of strong and rapid HNO<sub>3</sub> depletion, “June (R1-R2)” should be “June-August (R2)”.]

We indicate in the revised version: “... the strong and rapid HNO<sub>3</sub> depletion occurring in June (R2)”

[Section 4: Fig. 2 and its caption: More should be said about the agreement (or lack thereof) between the dashed and solid HNO<sub>3</sub> and the grey and red T lines when they both exist. Some readers may question why the PV approach is used, given the gaps in those curves. Also, perhaps this is just an optical illusion, but the solid blue line appears to be thicker in some years (2011, 2014, 2016, 2017) than in the others. If that is the case, then that also needs to be explained. In the caption, the level to which the stated PV value pertains (presumably 530 K) should be specified.]

The PV approach is indeed preferred for the calculation of the drop temperatures and the corresponding dates because it better delimits the inner vortex core. The time series in the 70–90°S Eqlat band are only represented for consistency with Fig. 1a. Even if the time series in the PV isocontour of  $-10 \times 10^{-5} \text{K} \cdot \text{m}^2 \cdot \text{kg}^{-1} \cdot \text{s}^{-1}$  or in the 70–90°S Eqlat band are very close during the Antarctic winter, differences in the drop temperature calculation might be found.

Only one blue solid line is plotted, hence, its width is the same over the IASI period.

The potential temperature at which the PV is taken (530 K) is now mentioned in the caption of the revised manuscript.

[L155: It is not appropriate to characterize the total HNO<sub>3</sub> depletion in the inner vortex as being the “coldest”.]

Indeed a word was missing here. It has been corrected: “... the regions inside the inner polar vortex where the temperatures are the coldest and the total HNO<sub>3</sub> depletion occurs.”

[L160: The wording in this sentence is garbled.]

It has been rewritten for clarity: “Note that the HNO<sub>3</sub> time series has been smoothed with a simple spline data interpolation function to avoid gaps in order to calculate the second derivative of HNO<sub>3</sub> total column with respect to time as the daily second-difference HNO<sub>3</sub> total column”.

[L162-163: 23 is more than “a few” days.]

It has been changed to: “...within some days...”

[L174-179 and Fig. 3 caption: The description of the figure is confusing. It is stated in both in L174-175 and the caption that the vertical red dashed line indicates, at 90S, the 10-year average of the drop temperatures (191.1 K) calculated from the HNO<sub>3</sub> second derivative time series in the area delimited by the  $-10 \times 10^{-6} \text{ K.m}^2.\text{kg}^{-1}.\text{s}^{-1}$  PV contour. It's not clear how a vertical line on a time series plot can represent a temperature value. Perhaps the authors meant to say the average date on which T dropped below the 195 K threshold at 90S? Moreover, the discussion above indicated that the value of 191.1 K was the average for the inner vortex (defined by either PV or EqL), not specifically at the South Pole (90S). In addition, the scale for the PV contour should be  $10^{-5}$ , not  $10^{-6}$ . Then in L176-177, it is stated that the “delay of 4-23 days between the maximum in total HNO<sub>3</sub> and the start of the depletion is also visible” – but how is a range of values (which arises from different years) visible in a climatological plot?]

The red dashed vertical line indeed represents the average drop temperature of 194 K calculated in the area delimited by the  $-10 \times 10^{-6} \text{ K.m}^2.\text{kg}^{-1}.\text{s}^{-1}$  PV contour; the position of the line matches the temperature of 194.2 K at 90°S. We agree that the representation of the averaged drop temperature is not clear. We now represent one isocontour for the averaged drop temperature and two vertical lines that encompass the dates on which the drop temperature is calculated. The scale for the PV contour has been corrected. We now state in the revised version that:

“The delay of some days between the maximum in total HNO<sub>3</sub> and the start of the depletion (see Fig. 2) is also visible in Fig. 3a.”

[Fig. 4: Very little discussion is devoted to this figure; it is merely noted (L177-178) that it shows the reproducibility of the IASI measurements of HNO<sub>3</sub> depletion from year to year. Since Fig. 1 already makes this point, the added value of Fig. 4 is not clear.]

The figure 4 clearly illustrates the reproducibility, from year to year, of the edge of the collar HNO<sub>3</sub> region delimited by the PV isocontour of  $-5 \times 10^{-5} \text{ K.m}^2.\text{kg}^{-1}.\text{s}^{-1}$  and of the region of the strong HNO<sub>3</sub> depletion delimited by the PV isocontour of  $-10 \times 10^{-5} \text{ K.m}^2.\text{kg}^{-1}.\text{s}^{-1}$  taken at 50 hPa, the pressure level considered in this study to derive the drop temperatures. This cannot be inferred from Figure 1 and this is the main reason why we think that Figure 4 has to be kept.

[Fig. 5: How relevant is the PV contour averaged over the May to October period, when the dates of the onset of HNO<sub>3</sub> depletion are May to June (or possibly July)? Why include August, September, and October in this average?]

We fully agree with that comment. Initially, the May-October period was chosen because it encompasses the dates of drop temperatures calculated in the region considered in Fig.5 (isocontour of  $-8 \times 10^{-5} \text{ K.m}^2.\text{kg}^{-1}.\text{s}^{-1}$ ). However, outside the polar vortex (defined by an isocontour of  $-10 \times 10^{-5} \text{ K.m}^2.\text{kg}^{-1}.\text{s}^{-1}$ ), drop temperatures are found much above the NAT formation temperature and they do not correspond to clear minima in the second derivative of HNO<sub>3</sub> total column with respect to time. Hence, considering that period for the PV contour is indeed not appropriate here.

We now represent, in the revised version, the PV contour over the 10 May to 15 July period that encompasses the dates of the onset of HNO<sub>3</sub> depletion inside the inner vortex core. Note that, on the contrary to the submitted version, we do not only consider the average of the PV over that period, but also the minima, which we find more representative of the drop temperature given the rapid displacement of the vortex: one bin can indeed be located inside the vortex one day and outside the vortex another day. Hence, that particular bin can be characterized by a depletion in HNO<sub>3</sub> with a specific drop temperature but an averaged PV larger than the value considered here to delimit the vortex core. The contour of  $-10 \times 10^{-5}$



$5\text{K}\cdot\text{m}^2\cdot\text{kg}^{-1}\cdot\text{s}^{-1}$  based on the minimum PV encountered over the 10 May to 15 July period as well as the isocontours of 195 K at 50 hPa for the averaged temperatures and the minima over the same period are also now represented in the revised Fig.5 and the distribution of the drop temperatures is much better described and explained in the revised version:

“The averaged isocontour of 195 K encircles well the area of HNO<sub>3</sub> drop temperatures lower than 195 K, which means that the bins inside that area characterize airmasses that experience the NAT threshold temperature during a long time over the 10 May – 15 July period. That area encompasses the inner vortex core (delimited by the isocontour of  $-10\times 10^{-5}\text{K}\cdot\text{m}^2\cdot\text{kg}^{-1}\cdot\text{s}^{-1}$  for the averaged PV), but is larger, and show pronounced minima (lower than  $-0.5 \times 10^{14} \text{ molec}\cdot\text{cm}^{-2}\cdot\text{d}^{-2}$ ) in the second derivative of the HNO<sub>3</sub> total column with respect to time (not shown here), which indicate a strong and rapid HNO<sub>3</sub> depletion.

The area enclosed between the two isocontours of 195 K for the temperatures, the averaged one and the one for the minimum temperatures, show higher drop temperatures and weakest minima (larger than  $-0.5 \times 10^{14} \text{ molec}\cdot\text{cm}^{-2}\cdot\text{d}^{-2}$ ) in the second derivative of the HNO<sub>3</sub> total column (not shown). That area is also enclosed by the isocontour of  $-10\times 10^{-5}\text{K}\cdot\text{m}^2\cdot\text{kg}^{-1}\cdot\text{s}^{-1}$  for the minimum PV, meaning that the bins inside correspond, at least for one day over the 10 May – 15 July period, to airmasses located at the inner edge of the vortex and characterized by temperature lower than the NAT threshold temperature. The weakest minima in the second derivative of total HNO<sub>3</sub> (not shown) observed in that area indicate a weak and slow HNO<sub>3</sub> depletion and might be explained by a short period of the NAT threshold temperature experienced at the inner edge of the vortex. It could also reflect a mixing with strong HNO<sub>3</sub>-depleted and colder airmasses from the inner vortex core. The mixing with these “already” depleted airmasses could also explained the higher drop temperatures detected in those bins. Finally, note also that these high drop temperatures are generally detected later (after the HNO<sub>3</sub> depletion occurs, i.e. after the 10 May – 15 July period considered here – not shown), which supports the transport, in those bins, of earlier HNO<sub>3</sub>-depleted airmasses and the likely mixing at the edge of the vortex.”

[L181: “the drop 50 hPa temperatures” should be “the 50 hPa drop temperatures”.]  
It has been corrected.

[L183: Technically, the isocontour represents  $-10$ , not  $\leq -10$ .]  
It has been corrected.

[L184-185: First, how does the range of dates corresponding to the onset of HNO<sub>3</sub> depletion reported here – mid-May to early July – relate to that reported (L163) in connection with Fig. 2, which was 17 May to 10 June? Does the difference in these estimates arise because the former is based on averages in  $1^\circ\times 1^\circ$  bins, whereas the latter is based on a vortex average within the PV contour? July seems rather late for the onset of PSC formation. Similarly, the range in 50 hPa drop T is quoted as 188.2 K to 196.6 K in L164, whereas here drop Ts vary over a wider range, from 180 to 210 K. The values at both extremes of this range are unrealistic. Indeed, the date and T ranges found in connection with Fig. 5 call into question the analysis method.]  
Indeed, the differences between the range in drop temperatures and corresponding dates shown in Fig.2 and in Fig.5 are simply due to the average (over the whole area delimited by a PV contour in Fig.2 vs in  $1^\circ\times 1^\circ$  bins within the PV contour).

See our response to comment [L186, L225] above about the extreme unrealistic values of drop temperature: The total HNO<sub>3</sub> columns over eastern Antarctica which show drop temperatures much above 195K might precisely be contaminated by strong surface emissivity features above ice; We have made this clear in Section 4.2 of the revised version:

“...emissivity features that are known to yield errors in the IASI retrievals. Indeed, bright land surface such as ice might in some cases lead to poor HNO<sub>3</sub> retrievals. Although wavenumber-dependent surface emissivity atlases are used in FORLI (Hurtmans et al., 2012), it is clear that this parameter remains critical and causes poorer retrievals that, in some instances, pass through the series of quality filters and affect the drop temperature calculation.”

[L189-196: The questionable results derived from this analysis cannot be pinned on biases in the ERA-Interim data. The statement is made that “Reanalysis data sets are, indeed, known to feature large uncertainties”, but the uncertainty in modern reanalysis temperatures (typically less than ~1 K) is by no means large enough to account for drop Ts as extreme as 180 and 210 K. The reliability of reanalysis temperatures in the polar lower stratosphere (including those from ERA-Interim) has been conclusively demonstrated in several recent papers, notably by Lawrence et al. [2018] and Lambert and Santee [2018]. Although both papers are cited here, their implications have apparently been overlooked.]

We fully agree with that remark that was also made by the referee #2. The discussion about the potential role of the uncertainty of the ECMWF reanalysis temperature on the drop temperature has been removed from the section, hence, this paragraph has been strongly revised accordingly:

“Biases in ECMWF reanalysis are too small for explaining the spatial variation in drop temperatures. Thanks to the assimilation of an advanced Tiros Operational Vertical Sounder (ATOVS) around 1998–2000 in reanalyses, to the better coverage of satellite instruments and to the use of global navigation satellite system (GNSS) radio occultation (RO) (Schreiner et al., 2007; Wang et al., 2007; Lambert and Santee, 2018; Lawrence et al., 2018), the uncertainties are reduced for several years. Comparisons of the ECMWF ERA Interim dataset used in this work with the COSMIC data (Lambert and Santee, 2018) found a small warm bias, with median differences around 0.5 K, reaching 0–0.25 K in the southernmost regions of the globe at ~68–21 hPa where PSCs form.”

[L197-199: This sentence is confusing and its intended meaning is unclear. It appears to be comparing apples (the spatial variability in drop T seen in the maps in Fig.5) to oranges (“natural” variations in PSC nucleation T, TTE, and PSC formation mechanism). Perhaps the authors meant the spatial variability in those parameters (and not the values themselves), but that is not how the sentence is constructed. In any case, further discussion of comparisons of Fig. 5 with previously published results is warranted.]

We here simply link the range in drop temperatures with that in PSCs nucleation temperatures (explained by a series of parameters – atmospheric conditions, TTE, type of formation mechanisms), not the spatial variability. The sentence has been rewritten for clarity:

“Except above some parts of Antarctica which are prone to larger errors, the overall range in the drop 50 hPa temperature for total HNO<sub>3</sub>, inside the isocontour for the 195 K temperature, typically extends from ~187 K to 195 K, which fall within the range of PSCs nucleation temperature at 50 hPa ...”.

Furthermore, note also that comparing the distributions of drop temperatures from IASI with PSC information from CALIPSO or MIPAS remains difficult given the difference in spatial coverage and, most importantly, the highly variable distribution of PSC types temporally (daily) and spatially (e.g. Höpfner et al., 2006; Lambert et al., 2012).

[L199-200: A number of other satellite data sets have captured gas-phase HNO<sub>3</sub> depletion (from both sequestration and denitrification) on similarly large scales.]

Indeed and numerous references about HNO<sub>3</sub> measurements in the polar regions during winter are mentioned in the manuscript where appropriate.

[Conclusions: L225-226: It is stated that “the range of drop temperatures is interestingly found in line with the PSCs nucleation temperature that is known, from previous studies, to strongly depend on a series a factors”. In fact, the derived range (180–210 K) is so large that it is arguably not in line with previous work, and it is therefore difficult to see how the IASI total column HNO<sub>3</sub> measurements provide added value (as stated in L203) to studies of Antarctic PSC formation and the interannual variability therein beyond that obtained from other satellite HNO<sub>3</sub> datasets.]

Please refer to our response to comment (L186, L225) above about the impact of the misrepresentation of the wavenumber-dependent surface emissivity above ice surface on the drop temperature calculation with some extreme values. Except for these extrema, the range of drop temperature in indeed in line with the PSCs nucleation temperature. This is now clearly mentioned in this section of the revised manuscript:

“Except for extreme drop temperatures that were found from year to year and suspected to result from unfiltered poor quality retrievals in case of emissivity issues above ice, the range of drop temperatures is interestingly found in line with the PSCs nucleation temperature”

[L230-231: The statement that this paper represents “the first time that such a large satellite observational data set of stratospheric HNO<sub>3</sub> concentrations is exploited to monitor the evolution HNO<sub>3</sub> versus temperatures” is wholly unsupported. In fact, there is a substantial body of literature on the relationship between HNO<sub>3</sub> and temperature, including studies of long-term vertically resolved datasets. In particular, Lambert et al. [2016] (which is cited in a number of places in this manuscript, but only in passing) examined 10 years of Aura MLS HNO<sub>3</sub> in the Antarctic winter vortex and its relationship to T – including temperature history (a factor that has been largely ignored here) and T with respect to TICE – as well as PSC composition as determined by CALIOP. In general, discussion of how the current results fit into the context of the findings from Lambert et al. [2016] and other relevant prior studies is inadequate.]

We wanted to highlight here the unprecedented exceptional spatial and temporal sampling of IASI for HNO<sub>3</sub> and certainly did not want to oversell the novelty of HNO<sub>3</sub>-temperature correlations. The sentence has been rewritten:

“We show in this study that the IASI dataset allows capturing the variability of stratospheric HNO<sub>3</sub> throughout the year (including the polar night) in the Antarctic. In that respect, it offers a new observational means to monitor the relation of HNO<sub>3</sub> to temperature and the related formation of PSCs.”

[L233-234: More explanation of how HNO<sub>3</sub> total column amounts could be used to inform PSC classification schemes is needed to justify this statement, especially given how spatially heterogeneous and layered PSCs have been shown to be.]

This sentence has been removed.

[Finally, in addition to the serious substantive issues enumerated above and in the formal reviews of the official referees, the manuscript suffers from the poor quality of the writing. If this paper were to be eventually accepted for publication, it would require extensive copy-editing to improve the English.]

We hope that with the changes made in the revised manuscript, which now also includes a comparison with MLS, G. Manney and M. Santee will not go against publication. A detailed reading of the paper has been done to correct the English linguistic/grammar mistakes.

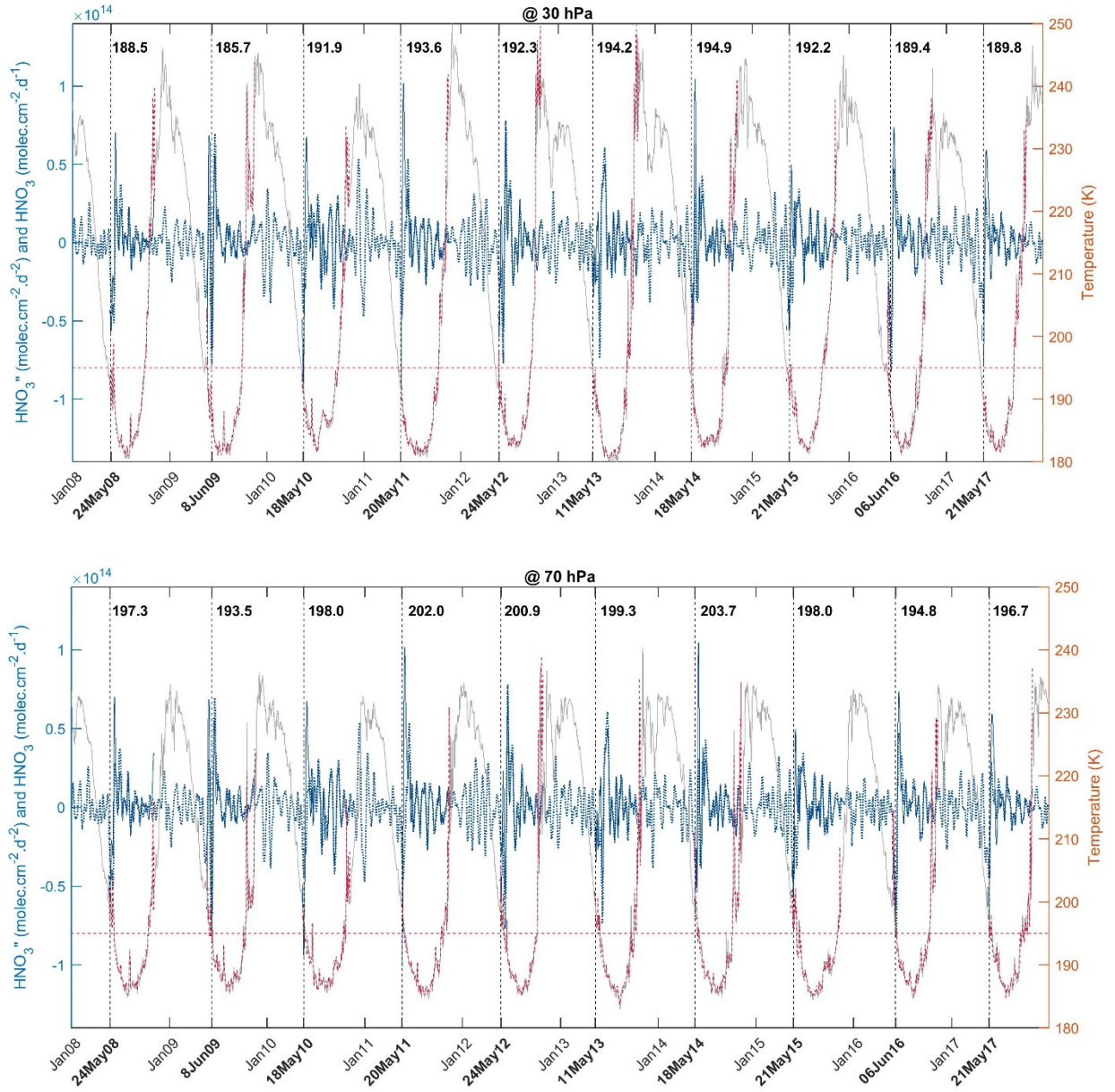


Figure 1. Same as Figure 2 of the manuscript but for the temperature at 30 hPa (top panel) and 70 hPa (bottom panel).



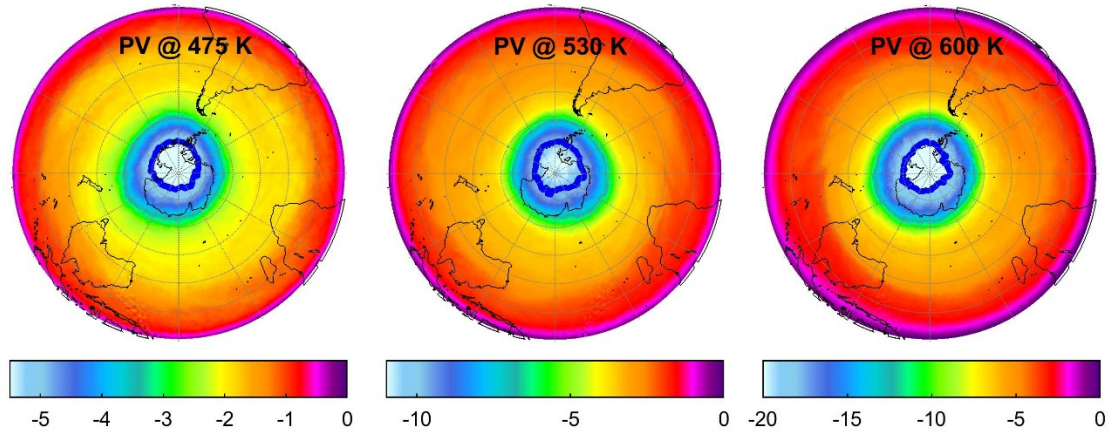


Figure 2. Spatial distribution of PV ( $\times 10^{-5} \text{ K.m}^2 \cdot \text{kg}^{-1} \cdot \text{s}^{-1}$ ) taken at three potential temperatures (475 K, 530 K and 600 K) over the range of the maximum IASI sensitivity, averaged over the period 15 May – 15 July for the year 2008. The blue lines represented the isocontours PV of  $-5.25 \times 10^{-5} \text{ K.m}^2 \cdot \text{kg}^{-1} \cdot \text{s}^{-1}$  (at 475 K),  $-10 \times 10^{-5} \text{ K.m}^2 \cdot \text{kg}^{-1} \cdot \text{s}^{-1}$  (at 530 K) and  $-19.4 \times 10^{-5} \text{ K.m}^2 \cdot \text{kg}^{-1} \cdot \text{s}^{-1}$  (at 600 K) averaged over the considered period.